# Oil & Natural Gas Technology

**DOE Award No.: DE-FE 0009963**

# Quarterly Research Performance Progress Report (Period ending 6/31/2013)

**Measurement and Interpretation of Seismic Velocities and Attenuations in Hydrate-Bearing Sediments**

**Project Period (10/1/2012 to 9/30/2015)**

Submitted by:
PI: Michael Batzle
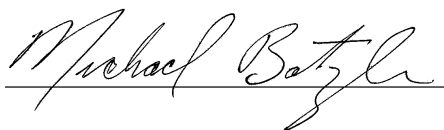Colorado School of Mines
DUNS #010628170.
1500 Illinois Street
Golden. CO 80401
e-mail: mbatzle@mines.edu
Phone number: (303) 384-2067
Submission Date: 7/31/2013

Prepared for:
United States Department of Energy
National Energy Technology Laboratory

**Office of Fossil Energy**

1

*Disclaimer:*

This report was prepared as an account of work sponsored by an agency of the United States Government. Neither the United States Government nor any agency thereof, nor any of their employees, makes any warranty, express or implied, or assumes any legal liability or responsibility for the accuracy, completeness, or usefulness of any information, apparatus, product, or process disclosed, or represents that its use would not infringe privately owned rights. Reference herein to any specific commercial product, process, or service by trade name, trademark, manufacturer, or otherwise does not necessarily constitute or imply its endorsement, recommendation, or favoring by the United States Government or any agency thereof. The views and opinions of authors expressed herein do not necessarily state or reflect those of the United States Government or any agency thereof.

*Abstract:*

Measurement and Interpretation of Seismic Velocities and Attenuations
in Hydrate-Bearing Sediments

Grant/Cooperative Agreement DE-FE 0009963.

Our research project is progressing well. Equipment is now in place and undergoing calibration. In addition, preparation and measurement procedures are being developed and tested. During the last quarter, we concentrated primarily on the CT scanner utilities and procedures to extract attenuation from ultrasonic data.

Initial pressure vessel to be used in the CT scanner is complete. This vessel must have the pressure and temperature capability to remain in the methane hydrate stability field. The vessel walls must permit significant Xray penetration. The signals must also not be degraded substantially either by the source-receiver geometry required. Our preliminary tests indicate that an image of porous material can be obtained from inside the vessel. However, the wall thickness forces the source-receiver into non optimum separation. Imaging will proceed with the current system, but ultimately, a vessel with thinner walls may be necessary.

We have initiated our measurements of attenuation (1/Q) of hydrate-bearing sediments. Initial measurements are based on ultrasonic compressional and shear waveforms. The high frequencies involved will provide the upper frequency limits on our 1/Q data. Acquisition and processing procedures measurements have been conducted on bead packs and the data are robust. An aluminum rod is being used as a reference material. The spectral ratio technique is being used to calculate attenuation. Results strongly depend on windowing and waveform similarity. Various coupling techniques and alternate standard materials are being tested.

## Contents:

*Appendices:*

Appendix I.

*Figures:*

**Executive Summary:**

Our project to measure the seismic attenuation and velocity as a function of texture and formation process is now well underway. During this reporting period, we concentrated on the 1. influence of the pressure vessel on the X-ray scan images (CT scans) and 2. attenuation estimates in the high (ultrasonic) frequency range.

In order to generate methane hydrates in sediments, we need to be in the elevated pressure range and low temperatures of the methane hydrate stability region. Although current work is concentrating on THF hydrates because of their easier formation pressure (atmospheric), developing the system for $CH_4$ hydrates is expected to be difficult, so equipment is now being built and tested. Initial pressure vessel to be used in the CT scanner is complete. This vessel must have the pressure and temperature capability to remain in the methane hydrate stability field. The vessel walls must permit significant X-ray penetration. The signals must also not be degraded substantially either by the source-receiver geometry required. Our preliminary tests indicate that an image of porous material can be obtained from inside the vessel. However, the wall thickness forces the source-receiver into non optimum separation. Imaging will proceed with the current system, but ultimately, a vessel with thinner walls may be necessary. Thinner walled ceramics have been obtained and are now being tested.

We have initiated our measurements of attenuation (1/Q) of hydrate-bearing bead packs and sediments. The current development are based on ultrasonic compressional and shear waveforms. The high frequencies involved will provide the upper frequency limits on our 1/Q data. Acquisition and processing procedures for the measurements have been conducted for both dry and water-saturated bead packs. The spectral ratio technique is being used to calculate attenuation. This ratio requires use of waves transmitted through a standard material with low losses. In this case, aluminum is used. Analysis over the entire waveform shows the common irregular results in the ratio due to contrasting waveform characteristics. Windowed data show a much more stable result. Various coupling techniques and waveform windowing techniques are now being further developed.

**Accomplishments**

I**. CT scanning vessel**

Imaging sediment samples containing methane hydrates using X-ray tomography (CT scans) is a primary goal of this project. Methane hydrates are stable only at low temperatures and high pressures. Thus, inside the CT scanner a vessel must be used to reach elevated pressures, yet still allow the X-rays to penetrate the sample. Other components will need to be attached to provide fluid flow and electronic feed-through. However, a proper pressure chamber must first be designed, fabricated, and tested.

One choice for the vessel would be a polymer with high strength. In this case, polycarbonate had several of the proper characteristics. However, an initial pure polycarbonate vessel proved too brittle. Fittings and attachments often produced cracks and led to pressure leaks. An alternative, related material is fiberglass filled polycarbonate. The vessel plus sealing components are shown in Fig. 1. The wall thickness is dictated by the pressures we are required to reach (2500 psi) and the strength of this material.

Initial CT scans were performed on bead packs to test the influence of both the vessel and the acquisition parameters forced by the presence of the vessel. The ¾ inch diameter sample was composed of 100 micron diameter glass beads. The scan was performed with a source-receiver separation of 6 cm as would be required when a vessel is present. The results are seen in Fig. 2. The beads themselves can be identified, but are very course and 'pixelated'. The image quality does not match the clear CT images shown in our previous quarterly report (Quarter 2 report, April 30). Some clarification can be accomplished with longer scan times and filtering. However, the effects of the non-optimal acquisition are apparent.

Scans of the sample inside the vessel are shown in Fig. 3. A similar blurred and pixelated image is seen. However, with the vessel, the image is downgraded. It is difficult to identify individual grains. Again, longer scanning times and filtering may enhance the image. In general, it appears that the size of the vessel, rather than the ability to transmit X-rays is important.

One solution to improving the images inside a vessel, would be to use a stronger material which would allow thinner vessel walls. We have thin-walled ceramic tubes (see Fig.4) now in place and will test these both for pressure containment and X-ray transmission characteristics. Fortunately, most of the other components of the pressure system can also be used on this material. Alternatively, aluminum oxide (sapphire) tubes are available require walls only a few millimeters thick. These will also be investigated.
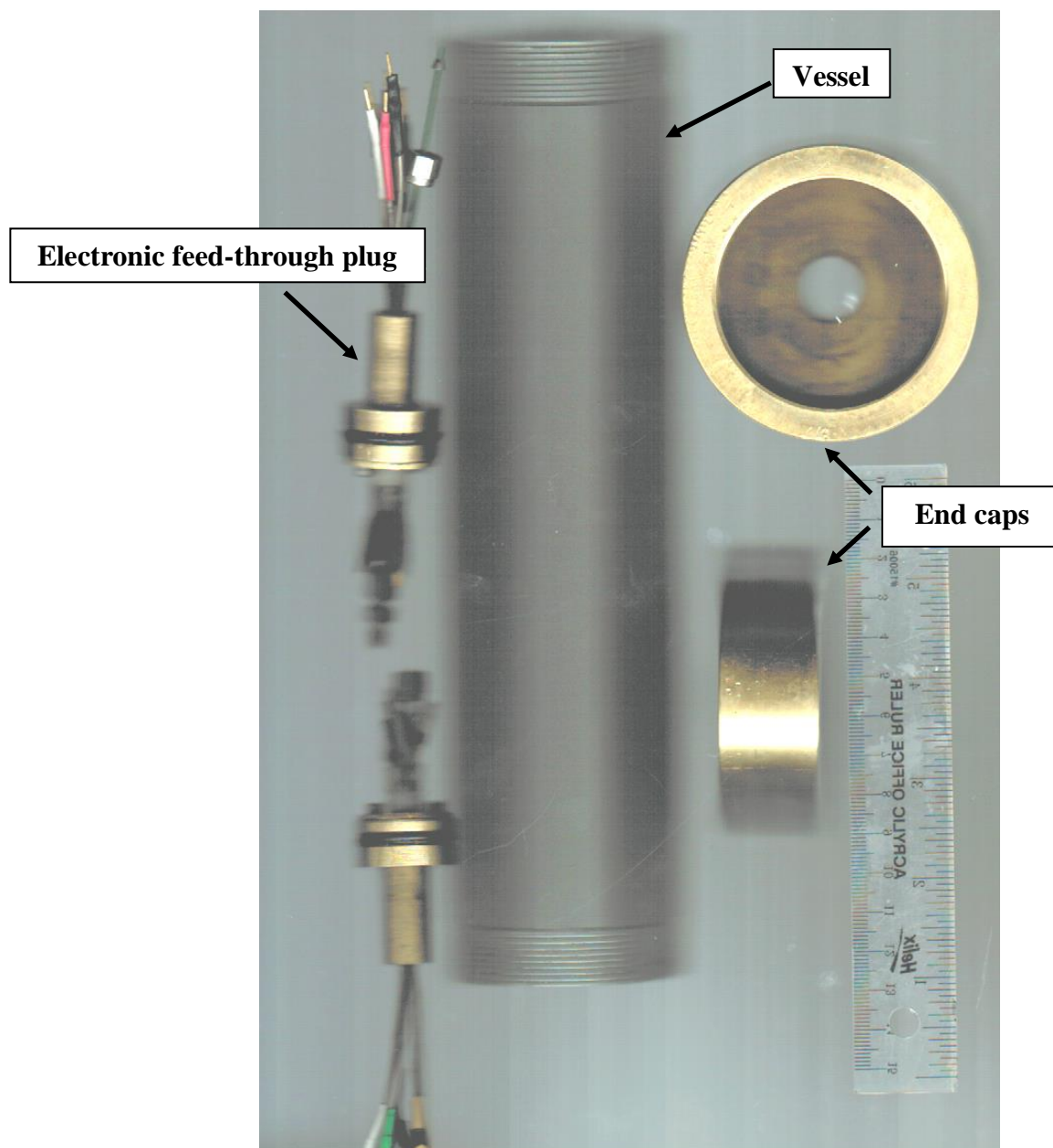
Fig. 1: Photograph of the glass-filled polycarbonate vessel and components.
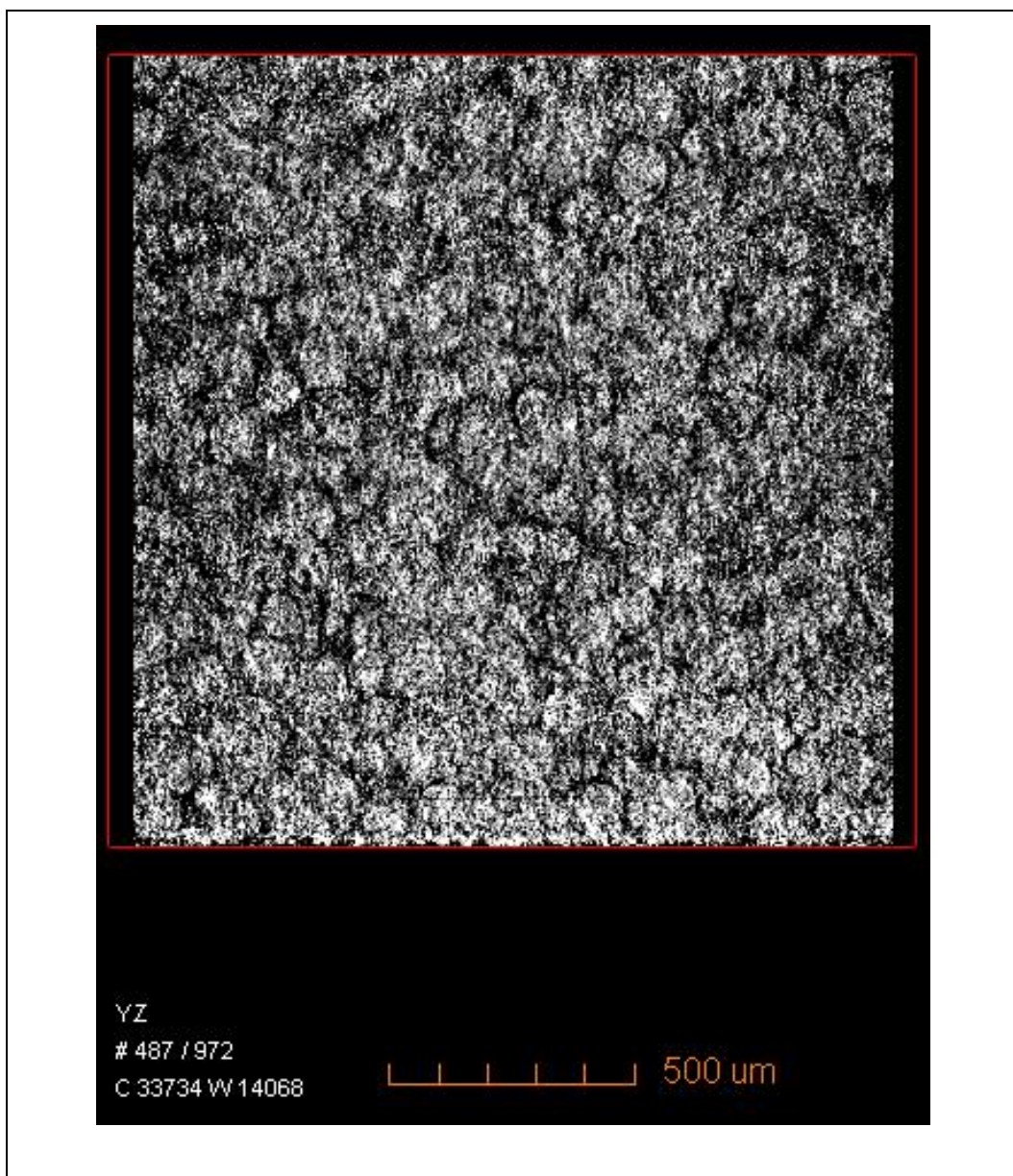
Fig. 2: CT scan of a 100 micron bead pack **without** the pressure vessel. Non-optimum geometries and acquisition parameters were used to mimic acquisition with the vessel in place.
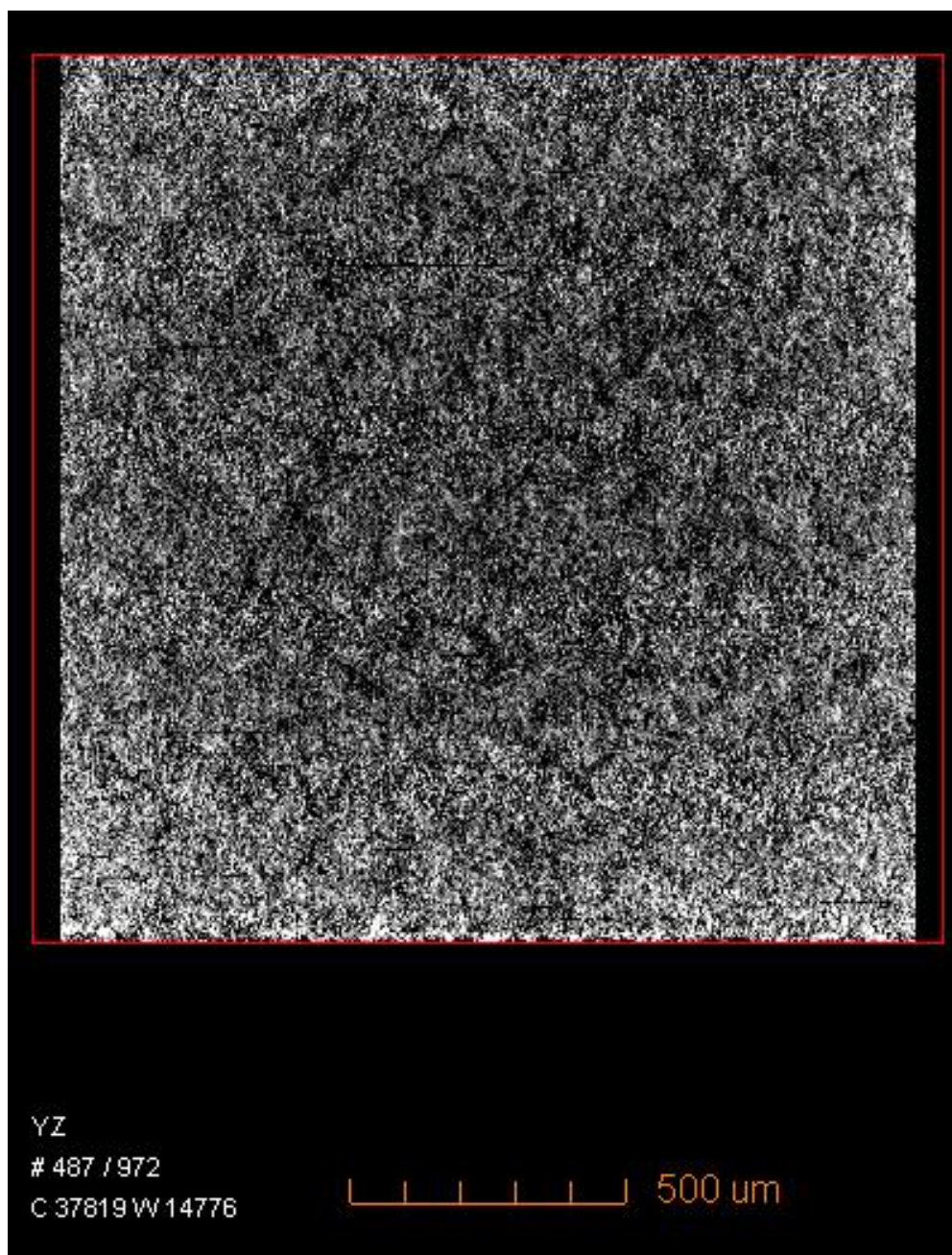
Fig. 3: CT scan with same geometry and acquisition parameters for sample inside the vessel.
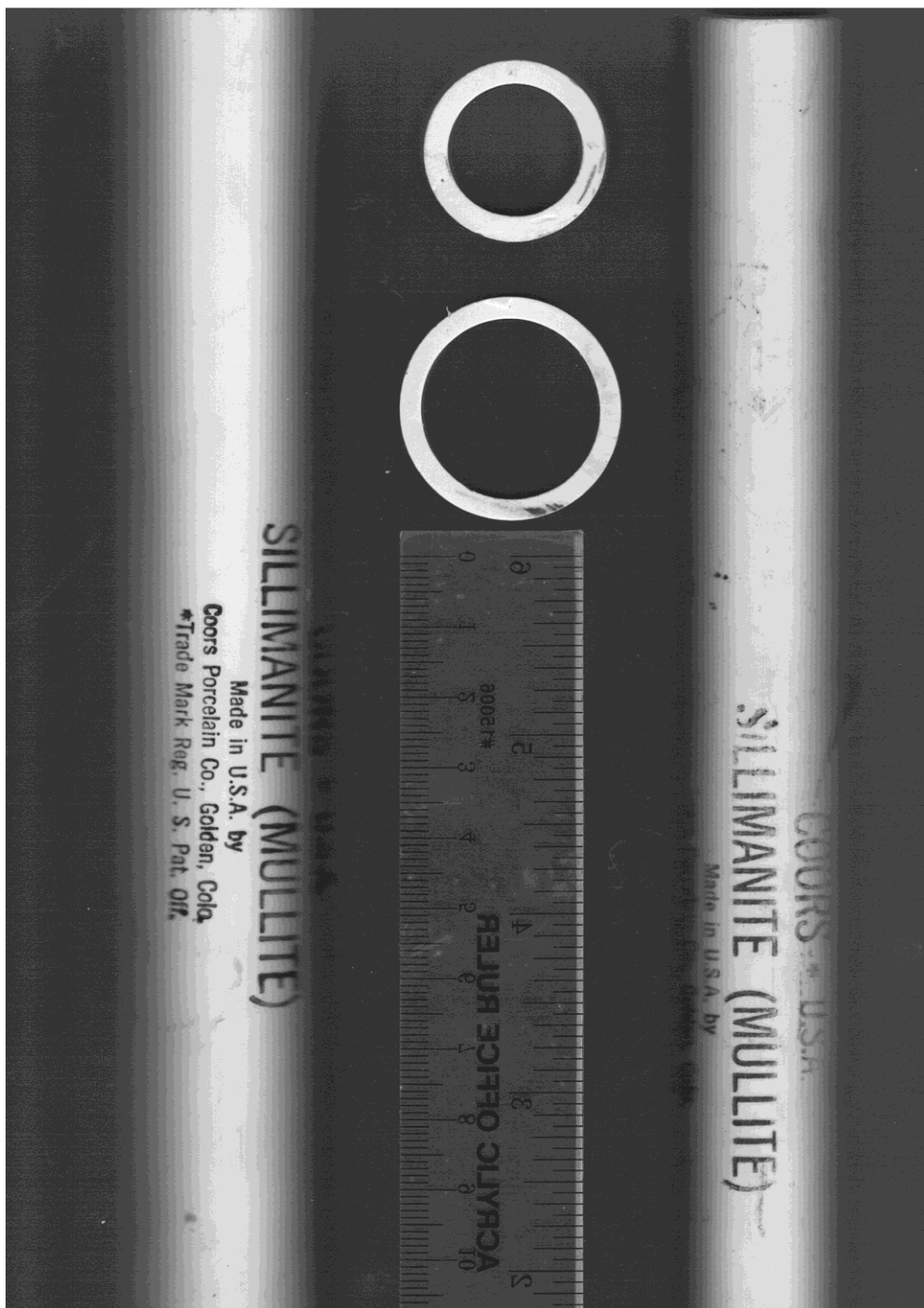
Fig. 4: Thin-walled sillimanite tubes to use as pressure vessel.

## II. Attenuation measurements

Elastic wave attenuation can be measured using several techniques. The 'low frequency' system actually collects data in both the seismic frequency range (3 to 2000 Hz) and in the ultrasonic range (0.1 to 1 MHz). This broad band is beneficial because attenuation peaks or loss mechanisms can then be identified.

The ultrasonic measurements are a wave propagation technique. As such, we can start with the classical description of wave amplitude (A)

$$A (x,t) = A_0 \exp[-\alpha t] \exp[i(kx - \omega t)] \tag{1}$$

Here x is distance, t is time, $\alpha$ is the attenuation coefficient, k is the real component of the wave number, and $\omega$ is frequency (radians/sec). We define the quality factor, Q as

$$1/Q = \alpha V/\pi f \quad \text{or} \quad \alpha = \pi f/VQ \tag{2}$$

Where V is velocity and f is frequency in Hz. If we assume the loss is constant over any wavelength, then comparing the observed loss at different frequencies can derive $\alpha$. Unfortuneately, the actual measured waveforms give frequency spectra that vary widely and have irregular amplitudes. This can be due in part to transducer characteristics, electronics, coupling, and sample geometry. To get around this problem, a common technique is the spectral ratio method (Johnston and Toksoz, 1981).

We can rewrite the amplitude as

$$A (x,t) = A(f) \exp[-(\pi f/VQ) \, x] \exp[i(kx - \omega t)] \tag{3}$$

Focusing on the loss component, the amplitude for a rock sample, $A_r$ will be

$$A_r (x,t) = A_r(f) \exp[-(\pi f/V_r Q_r) \, x] = A_r(f) \exp[-(\pi/V_r Q_r)fx] \tag{4}$$

If we have a standard material of the same size we will have

$$A_{sd} (c,t) = A_{sd}(f) \exp[-(\pi f/V_{sd}Q_{sd})x_0 f] \tag{5}$$

Where the subscript 'sd' refers to the standard and $x_0$ is the constant length. If we choose a standard material that is effectively lossless (such as aluminum), then $Q_{sd}$ is infinite and

$$A_{sd} (x_0,t) = A_{sd}(f) \quad \text{at some point } x_0 \text{ (or we could use time } t_0)$$

Taking the ratio of standard to rock to standard, we get

$$A_r/A_{sd} = A_r(f) \exp[-(\pi/V_r Q_r) \, cf] / A_{sd}(f) = A_r(f) / A_{sd}(f) \exp[-(\pi/V_r Q_r) \, x_0 f] \tag{6}$$

Taking the log of the ratio

$$\text{Ln}\,[A_r/A_{sd}] = \text{Ln}[A_{sd}(f)/\,A_r(f)] - (\pi/V_r Q_r)x_0 f \qquad (7)$$

Or, to simplify

$$\text{Ln}\,[R] = \text{Ln}[A_{sd}(f)/\,A_r(f)] - (\pi/V_r Q_r)x_0 f \;=\; C - (\pi/V_r Q_r)x_0 f \qquad (8)$$

If we approximate this by a line

$$y = C + mf$$

Then we extract $Q_r$ from the slope(m) of our line of $\text{Ln}[R]$ versus $f$ .

$$m \;=\; -(\pi x_0/V_r Q_r)$$

or $Q_r \;=\; -\pi x_0/m V_r$ \qquad (9)

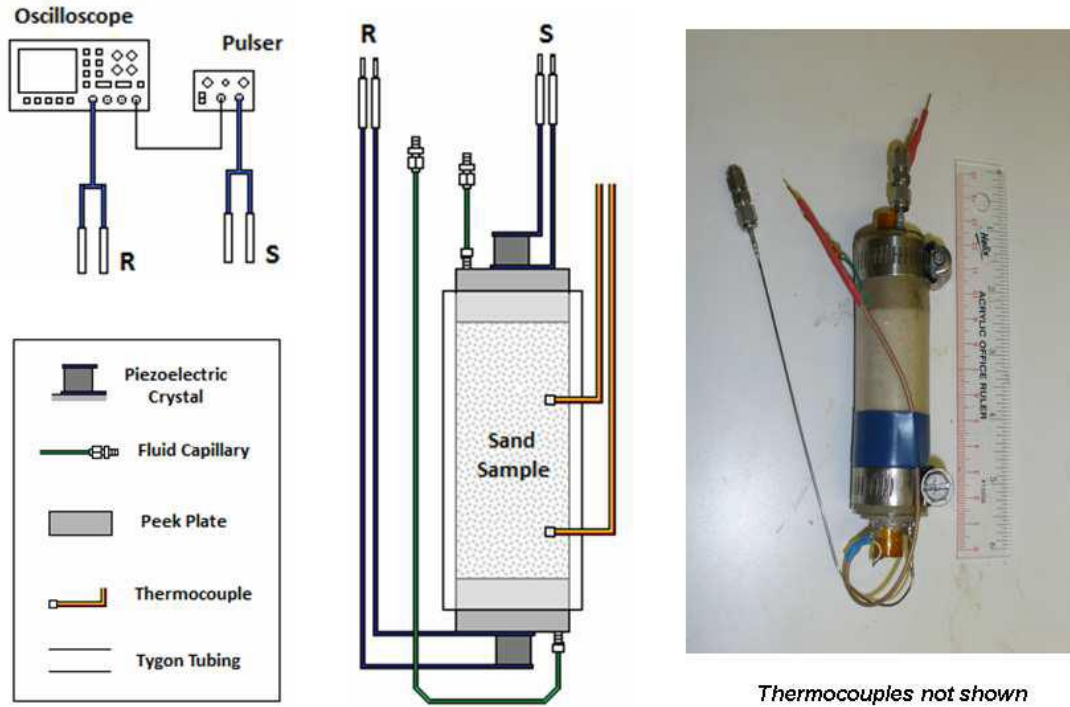To develop this for our application, we first use an ultrasonic assembly as shown in Fig.5.



Fig. 5. General transmission ultrasonic sample assembly (Rydzy and Batzle, 2008).

13

To start this kind of analysis, we collected p-waveforms through a dry bead pack as shown in Fig.6 (upper right). The spectrum is then calculated using a fast Fourier transform (fft) as shown in the upper right of Fig. 6. This is an extended waveform of 10,000 points and includes multiples, refracted, and converted wave contributions. These alternate energy paths explain the complex, spikey nature of the raw spectrum. To limit our examination to the pure direct arrival, the waveform is windowed around the first arrival using a Hanning window of 4096 points (Fig. 6, lower left). This yields a spectrum as seen in the lower right portion of Fig 6.

A similar analysis is performed for the s-waves in the dry bead pack as shown in Fig. 7. The s-wave has more contamination (converted p-waves) so even a windowed section around the first shear arrival produces a very irregular spectra (lower right in Fig.7). A similar data acquisition was then used for the bead pack saturated with water for the p-wave (figure 8) and s-wave (Fig.9). To clarify the arrivals, an expanded portion of the water-saturated p-wave is shown in Fig.10.
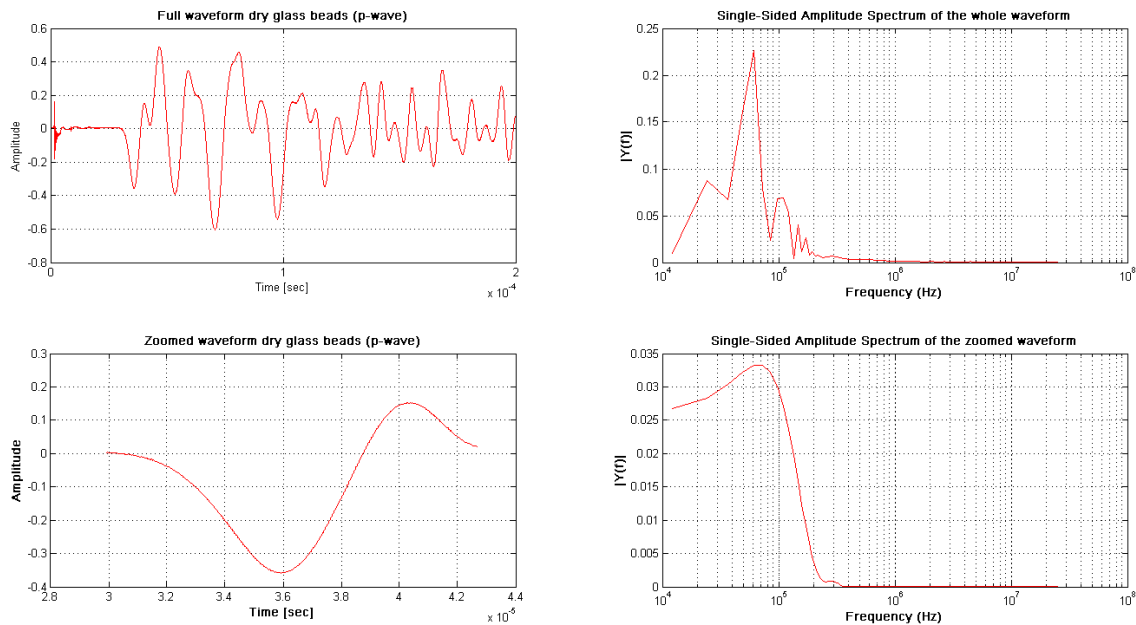


Fig. 6: upper left: recorded p-wave $P_C$ = 535 psi, $P_p$ = atmospheric pressure), upper right: calculated fft for the recorded waveform, lower left: one period of the p-wave arrival, lower right: calculated fft for the selected p-wave period

Fig. 7: upper left: recorded s-wave ($P_C$ = 535 psi, $P_p$ = atmospheric pressure), upper right: calculated fft for the recorded waveform, lower left: one period of the s-wave arrival, lower right: calculated fft for the selected s-wave period.
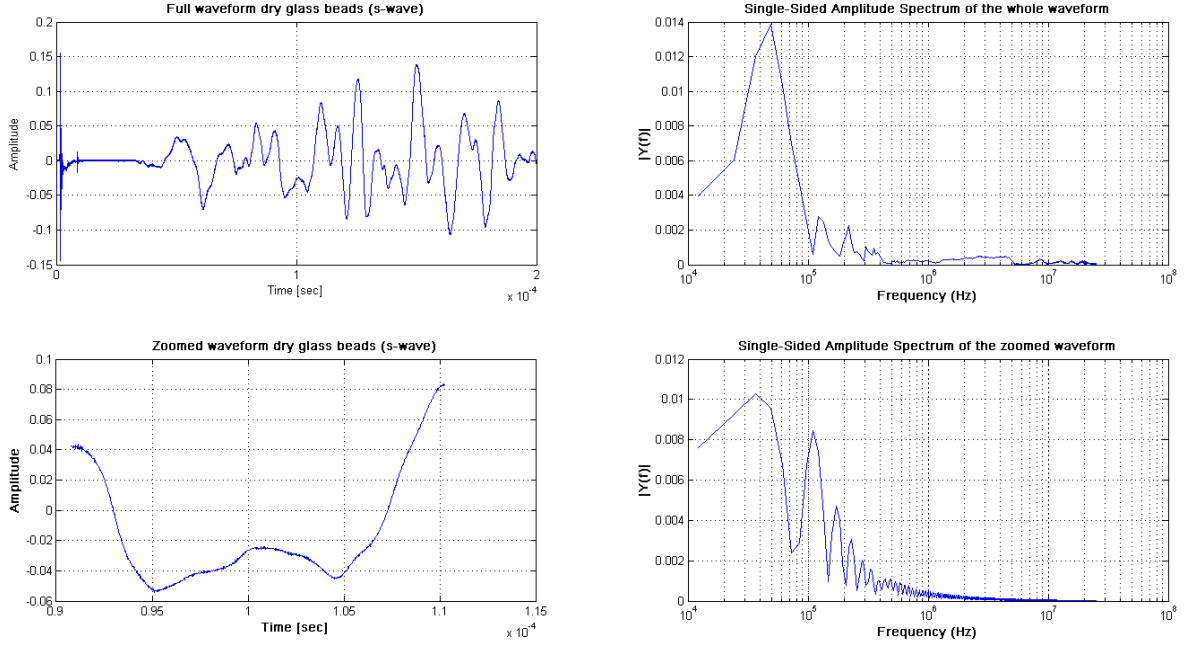


Fig. 8: upper left: recorded p-wave ($P_C$ = 735 psi, $P_p$ = 200 psi), upper right: calculated fft for the recorded waveform, lower left: one period of the p-wave arrival, lower right: calculated fft for the selected p-wave period

Fig. 9: upper left: recorded s-wave ($P_C$ = 735 psi, $P_p$ = 200 psi), upper right: calculated fft for the recorded waveform, lower left: one period of the s-wave arrival, lower right: calculated fft for the selected s-wave period
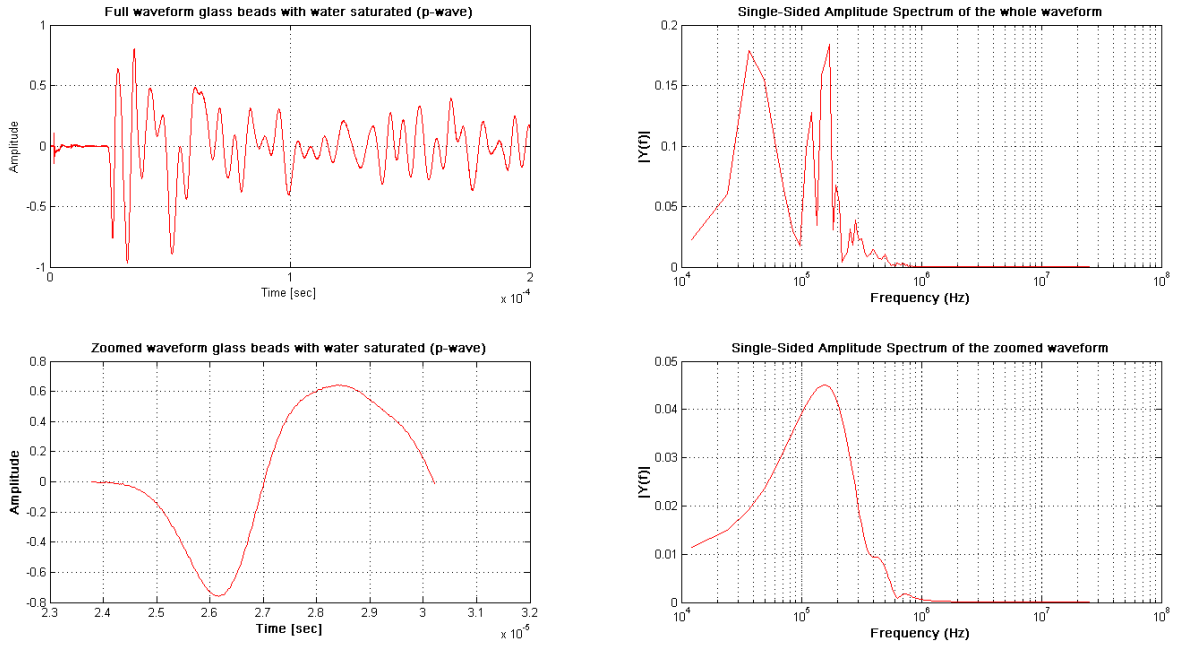


Fig. 10: Expanded portion of the p-wave, upper left: recorded p-wave ($P_C$ = 735 psi, $P_p$ = 200 psi), upper right: calculated fft for the recorded waveform, lower left: one period of the p-wave arrival, lower right: calculated fft for the selected p-wave period
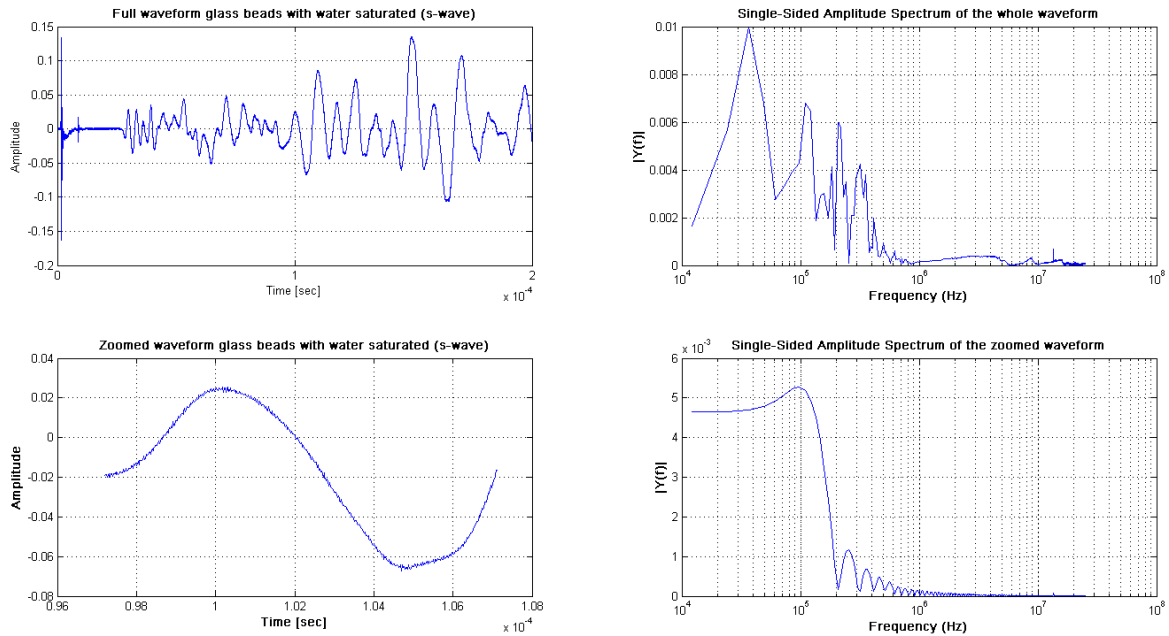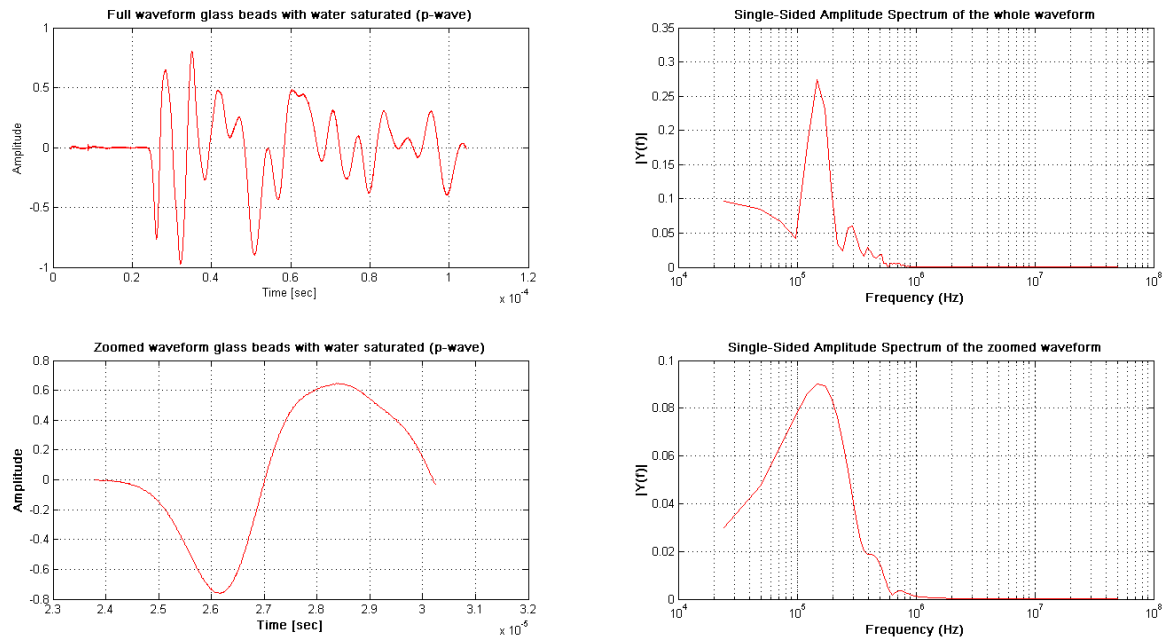
The previous figures have shown the waveforms and analysis in the windowed region of the first arrival. However, the spectra can be calculated as a function of time as the window is run across the entire waveform. An example is shown in Fig. 11 for the water-saturated pack. The browns and reds indicate high wave amplitudes within the window at that time. Using this kind of plot, we may be better able to identify the various contributing components to our complex waveforms.
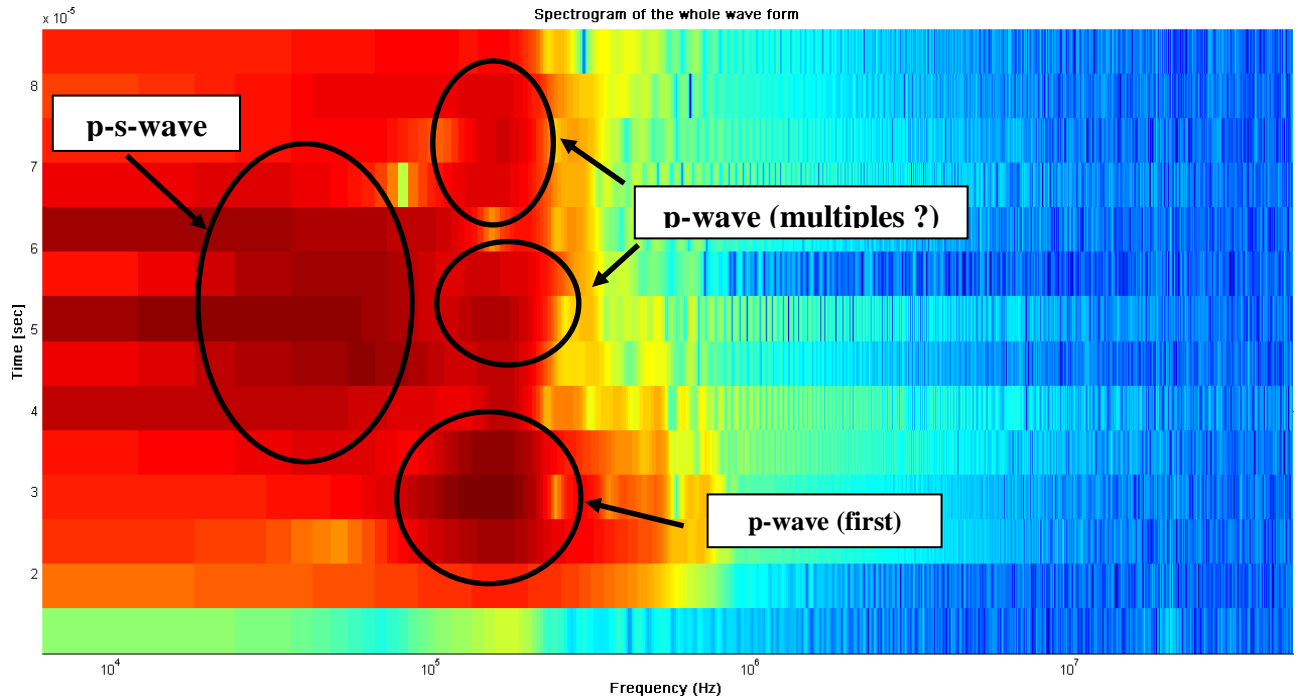


Fig. 11: Spectrogram of the water saturated glass bead sample ($P_c = 735$ psi, $P_p = 200$ psi). Darker reds indicate high amplitudes, blues indicate low amplitudes.

As indicated in equations 6 to 9, we need to compare our rock sample waveforms to waves through a standard, in our case, Aluminum. Fig.12 shows the full and windowed p - waveforms and spectral results from a trial on an aluminum standard at atmospheric pressure. Similar results for the s-wave are shown in Fig 13. The spectral ratio of the aluminum to rock (inverse of our ratio R in eqn. 8) is shown in Figures 14 and 15. The ratio is starting to provide us with a stable slope over a frequency range between about 200,000 Hz and 700,000 Hz. The windowed ratio (Fig.15 upper) giving a much better result than the ratio over the entire waveform (Fig. 15 lower).

Obviously, we need to do a more thorough job of collecting the sample and reference waveforms under the same environmental conditions and with acquisition parameters that result in similar waveforms.
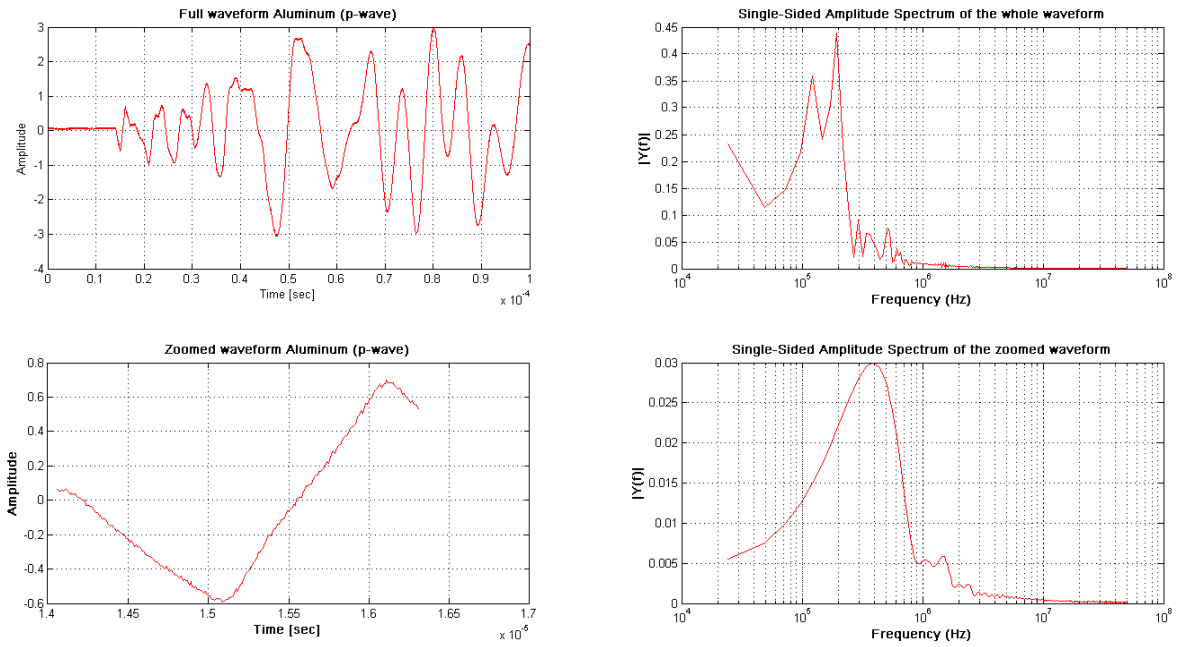
Fig. 12. P- waveform for traveling through an aluminum standard, left: recorded p- wave (@ atmospheric pressure), upper right: calculated fft for the recorded waveform, lower left: one period of the p-wave arrival, lower right: calculated fft for the selected p-wave period
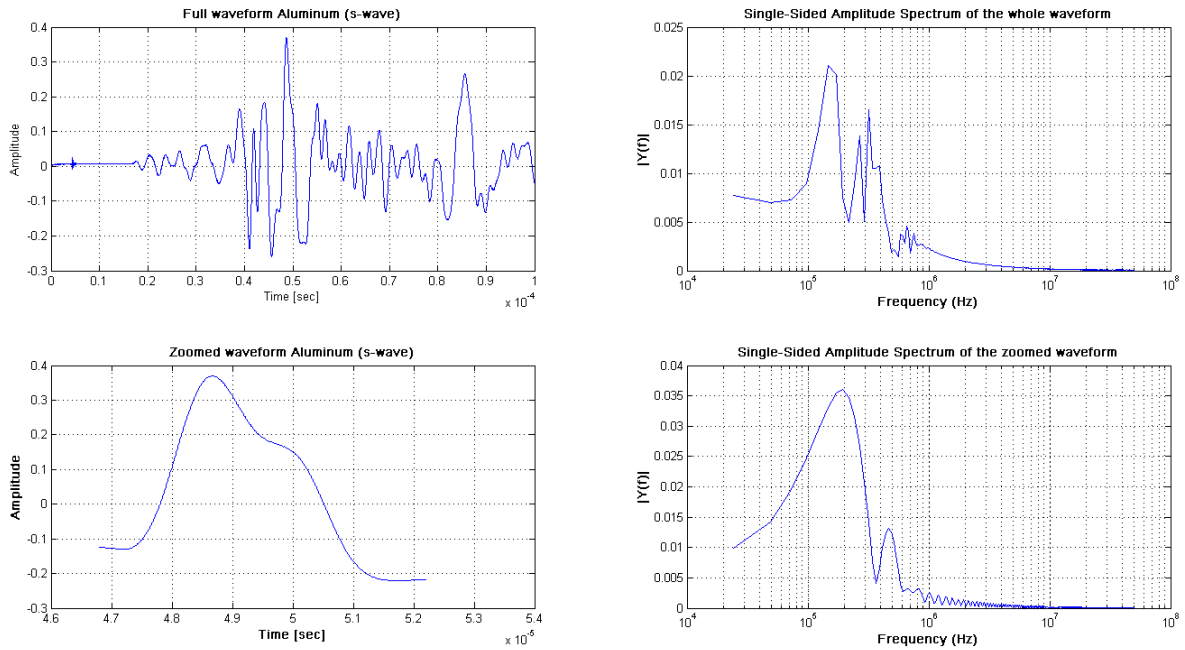


Fig. 13: s waveform for traveling through an aluminum standard, left: recorded s-wave (@ atmospheric pressure), upper right: calculated fft for the recorded waveform, lower left: one period of the s-wave arrival, lower right: calculated fft for the selected s-wave period

Fig. 14: FFT of the aluminum p-wave divided by the FFT of the water saturated glass bead p-wave sample, upper graph: one p-wave period, lower graph: the whole recorded waveform



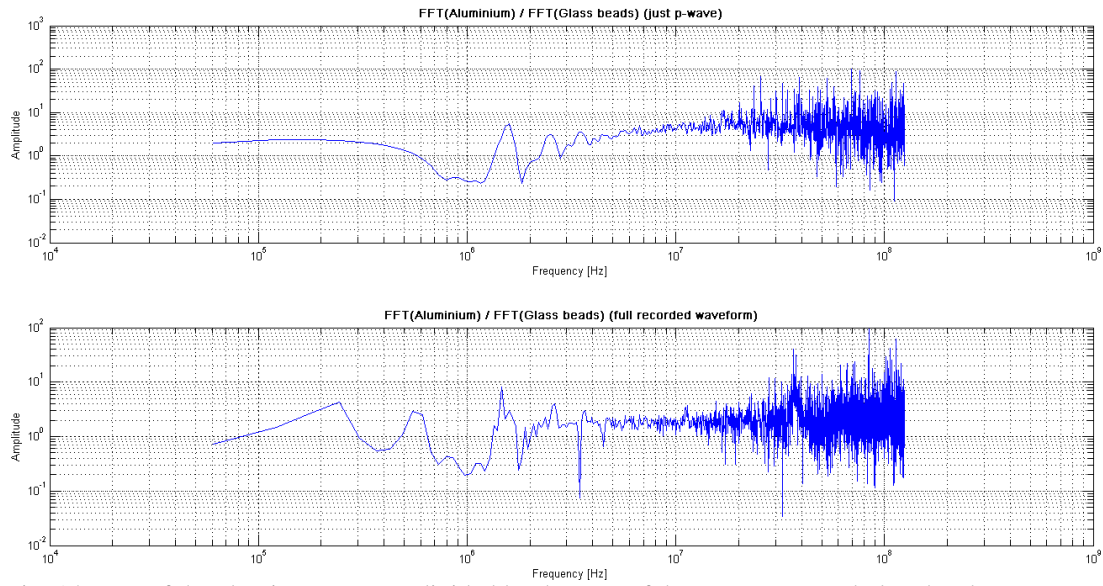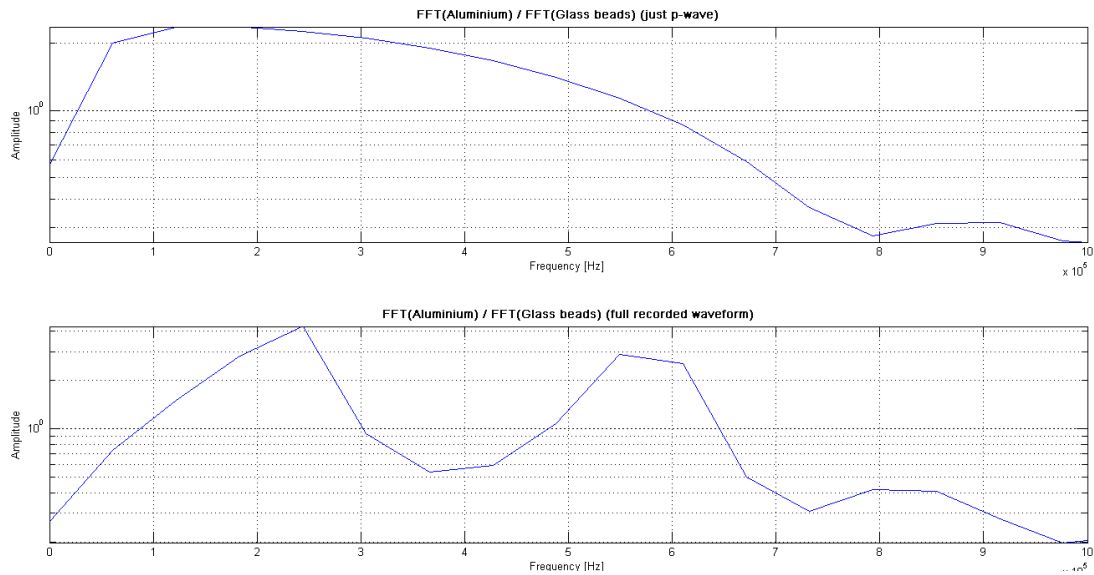Fig. 15: Expanded view of the fft of the aluminum p-wave divided by the FFT of the water saturated glass bead p-wave sample, upper graph: one p-wave period, lower graph: the whole recorded waveform

**Participants and Collaborating Organizations**

Name: George Radziszewski
Project Role: Research Faculty
Nearest person month worked this period: 1.5
Contribution to Project: Dr. Radziszewski spent his time establishing standards and procedures for running the MicroCT scanner .
Funding Support: "Organics, Clays, Sands and Shales (OCLASSH) consortium
Collaborated with individual in foreign country: No
Country(ies) of foreign collaborator: N/A
Travelled to foreign country: Yes
If traveled to foreign country(ies): Poland
Duration of stay: 2 weeks

Name: Mathias Pohl
Project Role: Graduate Student
Nearest person month worked this period: 3
Contribution to Project: Mr. Pohl prepared samples and collected ultrasonic data.
Additional Funding Support: N/A
Collaborated with individual in foreign country: No
Country(ies) of foreign collaborator: N/A
Travelled to foreign country: No
If traveled to foreign country(ies),
duration of stay: N/A

Name: Mandy Schindler
Project Role: Graduate Student
Nearest person month worked this period: 3
Contribution to Project: Ms Schindler prepared samples and collected CT data.
Additional Funding Support: N/A
Collaborated with individual in foreign country: No
Country(ies) of foreign collaborator: N/A
Travelled to foreign country: No
If traveled to foreign country(ies),
duration of stay: N/A

Name: Weiping Wang
Project Role: Laboratory Technician
Nearest person month worked this period: 0 (just started involvement)
Contribution to Project: Mr. Wang assisted in equipment fabrication
Additional Funding Support: N/A
Collaborated with individual in foreign country: No
Country(ies) of foreign collaborator: N/A

Travelled to foreign country: Yes
If traveled to foreign country(ies), N/A
duration of stay: N/A

Name: Michael Batzle
Project Role: Principle Investigator
Nearest person month worked: 1
Contribution to Project: Overall (dis)organization.
Funding Support: Academic faculty
Collaborated with individual in foreign country: No
Country(ies) of foreign collaborator: N/A
Travelled to foreign country: N/A
If traveled to foreign country(ies):

External Collaborations:
Dr. Tim Collett
US Geologic Survey
Denver, Colorado: (if foreign location list country)
Support: Data and guidance on interpretation and application
Tim continues to publish numerous papers on hydrate properties

**Changes / Problems**

The only significant change is the loss of Ms. Marisa Rydzy to graduation and employment. On a temporary basis, Ms. Mandy Schindler is conducting an internship in Houston, TX. Mr. Weiping Wang will assist, for the time being, in equipment fabrication and testing.

**Special Reporting Requirements**

None

**Budgetary Information**

Attached separately

**References**

Rydzy, M., and Batzle, M., 2009 Ultrasonic velocities in laboratory-formed gas-hydrate bearing sediments, Sageep annual meeting, Keystone CO.

Johnston, D., and Toksoz, N., 1981, Seismic Wave Attenuation, Geophysical Reprint Series, Number 2, SEG, Tulsa, OK

## Milestone Status

Measurement and Interpretation of Seismic Velocities and Attenuations in Hydrate-Bearing Sediments
DOE Award No.: DE-FE 0009963

| | Milestone Title / Description | Planned Completion Date | Actual Completion Date | Verification Method | Comments |
|---|---|---|---|---|---|
| 1 | Project Management Plan (PMP) | 1-Dec-12 | 28-Nov-12 | DOE acceptance | Complete and approved |
| 2 | Modifications to low frequency system | 1-Jun-13 | | | On schedule |
| 3 | Modeling established using EOS | 31-May-13 | | | On schedule |
| 4 | Property models of hydrates complete | 31-May-13 | | | On schedule |
| 5 | Logs acquired and database estab. | 31-Dec-13 | | | On schedule |
| 6 | THF hydrate grown in pressure vessel | 1-Jun-14 | | | On schedule |
| 7 | Methane hydrates from free gas phase | 31-Dec-14 | | | Planned |
| 8 | Methane hydrates from gas in solution | 30-Jun-15 | | | Planned |
| 9 | $CO_2$ replacing methane in hydrates | 30-Sep-15 | | | Planned |
| 10 | MXCT scans completed | 30-Sep-15 | | | Continuing |
| 11 | Effective media models complete | 30-Sep-15 | | | Planned |
| 12 | Comparison to in situ data complete | 15-Oct-15 | | | Planned |
| 13 | Information Dissemination | 31-Dec-15 | | | Continuing |